Manganese is a *Deinococcus radiodurans* growth limiting factor in rich culture medium

Francesca Borsetti°, Fabrizio Dal Piaz$, Federico D'Alessio•, Alessandra Stefan•^, Renato Brandimarti•, Anindita Sarkar£, Ankona Datta£, Alejandro Montón Silva§, Tanneke den Blaauwen§, Mucchi Alberto*, Enzo Spisni°, Alejandro Hochkoeppler•^#

° Department of Biology, Geology and Environmental Sciences, Via Selmi 3, 40125 Bologna (Italy)

• Department of Pharmacy and Biotechnology, Viale Risorgimento 4, 40136 Bologna (Italy)

$ Department of Medicine, University of Salerno, Via Giovanni Paolo II 132, 84084 Fisciano SA (Italy)

£ Department of Chemical Sciences, Tata Institute of Fundamental Research, Mumbai 400005 (India)

§ Bacterial Cell Biology & Physiology, Swammerdam Institute for Life Sciences, University of Amsterdam, Science Park 904, 1098 XH Amsterdam (The Netherlands)

*Department of Industrial Chemistry "Toson Montanari", University of Bologna, Viale Risorgimento 4, 40136 Bologna (Italy)

^ CSGI, University of Firenze, Via della Lastruccia 3, 50019 Sesto Fiorentino FI (Italy),

#To whom correspondence should be addressed:

Prof. Alejandro Hochkoeppler
Department of Pharmacy and Biotechnology
University of Bologna
Viale Risorgimento 4
40136 Bologna
Italy
Tel.: ++ 39 051 2093671
Fax: ++ 39 051 2093673
e-mail: a.hochkoeppler@unibo.it

Abbreviations: TGY: tryptone, glucose, yeast extract; BODIPY: boron dipyrromethene; TBS: Tris-Buffered-Saline; PBS: Phosphate-Buffered-Saline; EMCDD: electron multiplying charge-coupled-camera; CHAPS: 3-[(3-cholamidopropyl)dimethylammonio]-1-propanesulfonate; EDTA: ethylenediaminetetraacetic acid; IPG: immobilized pH gradient; DTT: 1,4-dithiothreitol; MS: mass spectrometry; LC-MS: liquid chromatography – mass spectrometry.

1

2 **ABSTRACT**

3

4

5 To understand the effects triggered by Mn^{2+} on *Deinococcus radiodurans*, the proteome patterns

6 associated to different growth phases were investigated. In particular, we tested under

7 physiological conditions the growth rate and the biomass yield of *D. radiodurans* cultured in

8 rich medium supplemented or not with $MnCl_2$. The addition to the medium of 2.5-5.0 µM $MnCl_2$

9 did neither alter the growth rate nor the lag phase, but significantly increased biomass yield.

10 When higher $MnCl_2$ concentrations were used (10-250 µM), biomass was again found to be

11 positively affected, although we did observe a concentration-dependent increase of the lag

12 phase. The *in vivo* concentration of Mn^{2+} was determined in cells grown in rich medium

13 supplemented or not with 5 µM $MnCl_2$. By atomic absorption spectroscopy we estimated 0.2

14 and 0.75 mM Mn^{2+} concentration in cells grown in control and enriched medium, respectively.

15 We qualitatively confirmed this observation using a fluorescent turn-on sensor designed to

16 selectively detect Mn^{2+} *in vivo*. Finally, we investigated the proteome composition of cells grown

17 for 15 or 19 h in medium to which 5 µM $MnCl_2$ was added, and we compared these proteomes

18 with those of cells grown in control medium. The presence of 5 µM $MnCl_2$ in the culture medium

19 was found to alter the pI of some proteins, suggesting that manganese affects post-translational

20 modifications. Further, we observed that Mn^{2+} represses enzymes linked to nucleotide

21 recycling, and triggers overexpression of proteases and enzymes linked to amino acids

22 metabolism.

23

24

INTRODUCTION

Deinococcus radiodurans is a Gram-positive bacterium, belonging to the Deinococcales order, whose members feature outstanding resistance to DNA-damaging agents [1]. Indeed, after its isolation from canned meat samples exposed to γ rays [2], *D. radiodurans* was the subject of quite a number of studies dealing with the competence of this bacterium in withstanding exposure to ionizing radiations. Early work was devoted to the investigation of the biochemical mechanisms exerted by *D. radiodurans* to repair damaged DNA [3-10]. Rather surprisingly, cells of *D. radiodurans* exposed to 14 kGy, and containing fragmented chromosomes, are able to reassemble their genomes within 6-7 h after radiation exposure [1]. Contrary to the vast majority of prokaryotes, *D. radiodurans* cells are polyploid, with the actual ploidy number being affected by growth phase [11] and culture medium [12]. Each genome copy consists of two chromosomes (containing 2.6 and 0.4 Mbp) and two plasmids, featuring $177 \cdot 10^3$ and $45.7 \cdot 10^3$ bp, respectively [13]. When this complex genome undergoes fragmentation, the essential 5'-3' exonuclease RecJ [14] produces 3' overhangs at the chromosomal/plasmid fragments, inducing the RecFOR-mediated loading of RecA onto DNA. The concerted action of RecA and DNA Polymerase DnaE recombine and extend the overlapping homologous fragments [15], according to a mechanism denoted ESDSA (Extensive Synthesis-Dependent Strand Annealing). While polyploidy is an obvious requisite for genome reconstruction competence, *D. radiodurans* does also feature additional and peculiar biochemical properties, responsible for genome integrity maintenance. Considering that ionizing radiations induce severe oxidative stress, it was realized that the radiation-resistance of *D. radiodurans* is mainly due to biochemical factors preserving the proteome of this bacterium from oxidation damages [1]. Among these biochemical factors, manganese is considered a relevant component, mainly because of the following observations: i) the cellular concentration of manganese in *D.*

radiodurans is high, ranging from 0.2 to 4 mM [16-18]; ii) *in vitro*, Mn^{2+}, in complex with phosphate ions, peptides, or amino acids, catalyzes the scavenging of superoxide radical [19, 20] and hydrogen peroxide [21]; iii) the depletion of Mn^{2+} from the culture medium triggers oxidative stress in *D. radiodurans* [22]. Therefore, it is not surprising that Mn^{2+} represents one of the main determinants of *D. radiodurans* ability to survive ionizing radiations. Remarkably, it was shown that the addition of 2.5 μM Mn^{2+} to solid medium was necessary for the growth of *D. radiodurans* cells in Petri dishes exposed to 50 Gy/hour [17]. In addition, it was also shown that a positive correlation exists between the level of radioresistance and the intracellular Mn/Fe molar ratio observed in different bacteria [17]. It should however be noted that the addition of Mn^{2+} to the growth medium is not necessarily beneficial to *Deinococcus radiodurans*. It was indeed shown that Mn^{2+} can induce a futile Embden-Meyerhof-Parnas pathway, and decreases the survival of *D. radiodurans* to UV light [23]. Moreover, the addition of Mn^{2+} to liquid cultures of *D. radiodurans* at early stationary phase triggers, in comparison with control cultures, an increase of biomass first, and a subsequent and pronounced decrease of live individuals in the bacterial population [24].

While the information relative to the protective role of manganese against ionizing radiations and oxidative damage is quite consistent, the effects that this metal can exert *per se* on the growth of *D. radiodurans* are poorly characterized. Early enough, it was recognized, and subsequently confirmed, that Mn^{2+} added to liquid cultures in rich medium at early stationary phase induces about 3 additional cell cycles and doubles the biomass yield [23-25]. Similar observations were reported for *Deinococcus geothermalis* [26]. Recently, the addition of Mn^{2+} to cultures of *D. radiodurans* at logarithmic phase in rich liquid medium was reported to increase biomass yield, although it did not affect the growth rate [27]. However, it was also reported that the addition of 5 μM Mn^{2+} to rich liquid medium decreased the growth rate of *D. radiodurans* [28], and that the effect of Mn^{2+} on the biomass yield is lower when compared with

4

75   the increase in population density triggered by Mg^{2+}, under optimal growth conditions [22].

76   Nevertheless, it was demonstrated that Mn^{2+} is essential for *D. radiodurans* growth. Indeed, no

77   significant growth was observed in a defined minimal medium (DMM) in the absence of Mn^{2+}

78   [17]. Moreover, it was shown that supplementing the medium with Mn^{2+} in the 0.25-500 nM

79   concentration interval did progressively increase both the growth rate and the biomass yield

80   [17]. No further effects were observed when the divalent cation was present at concentrations

81   higher than 500 nM.

82   A detailed study of the *D. radiodurans* growth kinetics as affected by the addition of Mn^{2+} to TGY

83   (<u>T</u>ryptone, <u>G</u>lucose, <u>Y</u>east extract) rich medium is presented here, along with a parallel

84   comparison of the proteomes of cells collected at late logarithmic and stationary phase, and

85   grown in standard or Mn^{2+}-enriched TGY medium. The observations accordingly obtained are

86   discussed, taking into account the intracellular Mn^{2+} levels, experimentally determined in the

87   different *D. radiodurans* populations considered.

88

89

90

91

92

93

94

MATERIALS AND METHODS

Strain and growth medium

Deinococcus radiodurans DSM 46620 was obtained from the Deutsche Sammlung von Mikroorganismen und Zellkulturen (DSMZ, Braunschweig, Germany), and grown in TGY medium (Tryptone, Glucose, and Yeast extract at 5, 1, and 3 g/L, respectively) at 30 °C under constant shaking (200 rpm).

Determination of growth in liquid media

The growth of *D. radiodurans* DSM 46620 in TGY liquid medium, supplemented or not with $MnCl_2$, was evaluated spectroscopically, and by cell and colony counting. Aliquots withdrawn from liquid cultures as a function of time were used to determine their Absorbance at 600 nm. In addition, the same aliquots were used for cell and colony counting, by means of a Thoma chamber (depth 5 μm, Poly-Optik GmbH, Blankenburg, Germany) and TGY solid medium, respectively.

Microscopy

From Petri dishes, 2 isolated colonies were used to obtain 2 independent pre-cultures in TGY medium at 30 °C. Each pre-culture was used after 24 h to inoculate 2 flasks containing 25 mL of TGY each. Morphology of cells from cultures incubated in TGY medium containing 0, 5, 25 or 250 μM $MnCl_2$ was evaluated 0, 12, 15 and 25 hours after dilution. Intracellular levels of Mn^{2+} were revealed using a turn-on BODIPY-based fluorescent probe, the selectivity of which was previously described [29]. From cultures incubated in TGY medium containing 0, 5, 25, or 250 μM $MnCl_2$, a 1mL aliquot was taken and washed 3 times with TBS to remove the excess of $MnCl_2$ of the medium. The BODIPY-based Mn^{2+} sensor (70 μM) was added to each sample and incubated at 30 °C for 15 minutes. Samples were washed 3 times with PBS and imaged with a

119   Nikon Eclipse T1 microscope (Nikon Plan Fluor × 100/1.30 Oil Ph3 DLL objective) coupled to

120   an EMCCD camera. Images were analyzed using ImageJ software [30].

121   ***Sample preparation for 2D-PAGE***

122   In order to remove lipids and carotenoids from the more external layers, frozen cells from 25

123   mL of cultures were incubated with absolute ethanol for 15 minutes on ice. Cells suspensions

124   were then centrifuged at 16,000 g for 10 minutes and pellets were resuspended in 0.5 mL of

125   lysis buffer (7 M Urea, 2 M Thiourea, 4% w/v CHAPS, 50 mM DTT, 1 mM Sodium EDTA, 20 mM

126   Tris base, IPG buffer 3-10, pH 6.8), containing Protease Inhibitors Cocktail (GE Healthcare,

127   Piscataway, USA). Cells were sonicated for 2.5 minutes (cycles of 15 seconds with 1 minute

128   intervals) on ice using a Branson Digital Sonifier (Thermo Fisher Scientific, Waltham, USA) at

129   20 % of amplitude, and then centrifuged for 20 minutes at 16,000 g to pellet insoluble

130   components. Supernatants were collected, and protein concentration was determined using

131   the Bradford Quick Start™ reagent (BioRad, Hercules, USA). Then, about 500 μg of total

132   proteins from each sample were purified by ReadyPrep 2D Clean Up kit (BioRad), according to

133   manufacturer's instructions, and precipitated proteins were resuspended in lysis buffer. The

134   protein concentration of purified samples was determined as above, and aliquots were stored

135   at -80°C.

136   ***2D Electrophoresis***

137   For each sample, a 190 μg of total protein was diluted to 250 μl with rehydration solution,

138   containing 7 M Urea, 2 M Thiourea, 4 % CHAPS, 0.5 % IPG buffer 4-7 (GE Healthcare), 1.2 %

139   DeStreak™ reagent (GE Healthcare) and Bromophenol Blue in trace amount. Immobiline Dry

140   Strips gels (pH 4-7, 11 cm, GE Healthcare) were passively rehydrated overnight in strip holders

141   and electrofocused in Ettan IPGphor 3 (GE Healthcare). Focusing (20000 V•hrs) was carried

142   out at 50 μA/strip and 15 °C, 500 V (5 h), 1000 V (2 h), gradient to 8000 V, 8000 V to end. IPG

143   strips were incubated for 15 minutes in equilibration buffer (6 M Urea, 30 % v/v glycerol, 2 %

144 w/v SDS, 75 mM Tris HCl buffer, pH 8.8) containing 130 mM DTT, and then for further 15

145 minutes in equilibration buffer containing 135 mM Iodoacetamide. Strips were sealed in place

146 on top of Criterion Precasted Gels–Any kD (BioRad) using 1 % w/v agarose in running buffer

147 with trace amount of bromophenol blue. The second dimension was performed using a

148 Criterion electrophoresis cell (BioRad) under constant current (30 mA/gel and 250 V max).

149 Gels were fixed in 40 % v/v Methanol and 10 % v/v Acetic Acid solution for 2 hours, and then

150 stained overnight with Colloidal Coomassie Blue G solution. After several washes, gels were

151 scanned with Pharos-FX system and analyzed using Proteomweaver™ software (both from

152 BioRad).

153 ***Preparation of samples for mass spectrometry***

154 Spots were excised from gels and treated as reported by Shevchenko et al. [31]. Briefly, spots

155 were destained in 50 mM ammonium bicarbonate in acetonitrile (ACN) and dehydrated with

156 pure ACN. Samples were then reduced with 10 mM DTT, and alkylated with 55 mM

157 iodoacetamide in 100 mM ammonium bicarbonate (Millipore-Sigma, St. Louis, USA). After

158 dehydration in ACN, gel pieces were equilibrated at 4 °C in solution A (10 mM ammonium

159 bicarbonate, 10 % ACN) containing 13 ng/µl of porcine trypsin for MS (Millipore-Sigma) for 2

160 hours, and then incubated at 37 °C overnight. After spinning, supernatants were harvested and

161 gel pieces were covered by extraction solution (5 % formic acid in ACN). After 15 minutes of

162 incubation at 37 °C, supernatants from this step where pooled to the corresponding

163 supernatants of the previous step and dried in SpeedVac (Savant™).

164 ***Mass spectrometry***

165 Separation of peptides were performed as previously described [32]. The resulting peptides

166 were analyzed by LC-MS/MS using an Orbitrap XL instrument (Thermo Fisher Scientific)

167 equipped with a nano-ESI source coupled with a nano-Acquity capillary UPLC (Waters, Milford,

168 USA). Briefly, peptides were separated with a capillary BEH C18 column (0.075 x 100 mm, 1.7

169 μM, Waters) using aqueous 0.1 % formic acid (A) and CH_3CN containing 0.1 % formic acid (B)

170 as mobile phases. Peptides were eluted by means of a linear gradient from 5 to 50 % of B in 90

171 minutes, at a 300 nL/minute flow rate. Mass spectra were acquired over an *m/z* range from 400

172 to 1800. To achieve protein identification, MS and MS/MS data underwent Mascot Search

173 Engine software analysis to interrogate the National Center for Biotechnology Information non

174 redundant (NCBInr) protein database. Parameters sets were: trypsin cleavage;

175 carbamidomethylation of cysteines as a fixed modification, and methionine oxidation as a

176 variable modification; a maximum of two missed cleavages; false discovery rate, calculated by

177 searching the decoy database, was set at 0.05.

178 ***Atomic absorption spectroscopy***

179 The concentration of Mn^{2+} in liquid samples was determined using a Varian Spectra AA•100

180 GTA110 Spectrometer, equipped with a graphite furnace. The calibration curve was obtained

181 by dilution of a commercial standard (1000 ppm, Carlo Erba, Cornaredo, Italy) to 20, 40, 60,

182 and 80 ppb. For the analysis of glucose, tryptone and yeast extract, 1 g of each sample was

183 individually dissolved in 24.75 mL of ultrapure H_2O to which 250 μL of HNO_3 was added. The

184 solutions accordingly obtained were then analyzed. For the estimation of Mn^{2+} in *D.*

185 *radiodurans* cells, aliquots of liquid cultures (1 mL) were centrifuged and the resultant pellets

186 were washed twice with ultrapure H_2O. Finally, the washed pellets were resuspended and

187 subjected to analysis.

188

189

190

RESULTS AND DISCUSSION

Growth of Deinococcus radiodurans in TGY medium enriched with Mn^{2+}

As a first test, we assayed the growth of *Deinococcus radiodurans* at 30 °C in TGY medium to which 0, 2.5, 5, 10, 25, or 250 µM Mn^{2+} was added. Accordingly, we spectroscopically determined the growth kinetics of the corresponding bacterial populations, of which the majority did reach the stationary phase within 35 h (Fig. 1a). The addition of Mn^{2+} to the medium positively affected the biomass yield, and at concentrations ≥ 10 µM increased the time length of the lag phase. In particular, when compared to the control, all the cultures grown in manganese-enriched TGY medium featured a higher population density at the end of the time interval considered (Fig. 1a). When the lag phase is analyzed, 10, 25 and 250 µM Mn^{2+} did significantly delay the onset of growth, by about 10, 15, and 20 h, respectively (Fig. 1a). In contrast, the addition of 2.5 or 5 µM manganese to TGY medium did neither alter the lag phase nor the growth rate, but increased the biomass yield about 1.5 fold when compared to the control culture (Fig. 1a). We further tested this effect by comparing control and manganese-supplemented cultures. To this aim, 3 single colonies of *D. radiodurans* were used to inoculate 3 independent pre-cultures, whose growth was performed in TGY medium at 30 °C for 48 h. Each pre-culture was then diluted in TGY and in the same medium to which 5 µM Mn^{2+} was added, and the 6 cultures accordingly obtained were incubated for 15 h at 30 °C, under constant shaking. Based on the determined growth kinetics of each culture, we observed significant higher biomass yields in the manganese-supplemented cultures (Supplementary Fig. S1). To better define the stimulation of *D. radiodurans* growth exerted by Mn^{2+}, the biomass yield by cell and colony counting, after 19 h of growth at 30 °C, was estimated. When the number of individuals per unit volume was determined using a Thoma chamber, we observed that the addition of Mn^{2+} doubled the population density (Fig. 1b). A similar magnitude of the effect

216   induced by manganese was also observed by colony counting (Fig. 1b). Not surprisingly, the

217   absolute values were in this case slightly lower than those relative to the number of total cells

218   per unit volume, for both the control and the manganese-supplemented cultures. It is important

219   to note that the addition of manganese to TGY medium, besides inducing a significant increase

220   in biomass yield (Fig. 1b), did not dramatically affect the partition of the bacterial population

221   among single cells, diads, and tetrads (Fig. 2). The only significant effect observed was indeed

222   a slight increase of the occurrence of diads and tetrads in the population grown in manganese-

223   supplemented medium (Fig. 2).

224   The formulation of a defined minimal medium (DMM) for *Deinococcus radiodurans* [33] was a

225   mandatory step to recognize manganese as essential for the growth of this microorganism [17].

226   The effect on *D. radiodurans* growth eventually induced by the addition of manganese to rich

227   media was tested under different conditions. Generally, high concentrations (100-500 μM) of

228    $MnCl_2$ were chosen to inoculate a TGY-enriched medium [24, 28], or to supplement TGY at

229   stationary [23-25] or logarithmic phase [27]. Nevertheless, Chou and Tan observed that

230   concentrations of Mn^{2+} in the 0-2.5 μM interval suffice to increase the biomass yield of *D.*

231   *radiodurans* in rich medium [24]. Overall, these observations agree in suggesting that the

232   concentration of manganese in rich media is sub-optimal when the biomass yield is considered.

233   Despite this agreement, conflicting evidence was reported about the effect of Mn^{2+} towards the

234   growth kinetics of *D. radiodurans* in rich media. The divalent cation was indeed shown to be

235   ineffective [23, 27] or detrimental [23, 25, 28] towards the growth rate. We reported here that

236   concentrations of $MnCl_2$ ranging from 2.5 to 250 μM did not significantly alter the growth rate

237   of *D. radiodurans*, albeit triggering higher biomass yields (Fig. 1a). However, we observed a

238   consistent increase of the time length of the lag phase as the TGY medium was supplemented

239   with manganese at concentrations higher than 10 μM (Fig. 1a). The divergence between our

240   and previous observations is quite likely due to the method we used to prepare the cultures:

241 contrary to what customarily done [23, 28], we did not pre-culture cells in manganese-enriched

242 medium, but we instead used a single pre-culture grown in TGY medium, and this single pre-

243 culture was subsequently split in 2 cultures, in TGY and in TGY supplemented with MnCl$_2$,

244 respectively. This means, in turn, that the cells we grew in TGY Mn^{2+}-enriched medium were

245 adapting to the presence of the divalent cation, most likely by expressing proteins useful to deal

246 with the presence of manganese. In our view, this was important to obtain meaningful samples

247 for protein extraction and mass spectrometry, with the aim to identify components of the

248 proteome responsible for the positive response of *D. radiodurans* to manganese.

249 **Mn^{2+} levels in *Deinococcus radiodurans* cells**

250 To evaluate the propensity of *D. radiodurans* cells to accumulate Mn^{2+}, we analyzed by atomic

251 absorption spectroscopy the concentration of this divalent cation both in TGY medium and in

252 whole cells. First, we determined the concentration of Mn^{2+} in the 3 components of TGY, *i.e.*

253 tryptone, yeast extract, and glucose. Using solutions at 40 g/L of each compound, we were able

254 to determine 3.05 ± 0.09, and 2.19 ± 0.08 µg/g (ppb) of Mn^{2+} in tryptone and yeast extract,

255 respectively. The content of the divalent cation in glucose was below the detection limit of our

256 procedure, equal to 0.4 µg/g. Accordingly, and considering the composition of TGY (Tryptone,

257 Glucose, and Yeast Extract at 5, 1, and 3 g/L, respectively), the concentration of Mn^{2+} in the

258 medium was equal to 21.82 µg/L, *i.e.* 0.4 µM. The manganese concentration was then

259 determined in whole cells grown for 15 or 19 h in TGY, or in the same medium to which 5 µM

260 Mn^{2+} was added. To estimate the manganese concentration *in vivo*, the number of cells of each

261 sample was counted with a Thoma chamber, and the volume of a single cell was assumed as

262 equal to 8 µm^3. According to this assumption, the data obtained for cells cultured for 15 h

263 (Supplementary Fig. S2a) correspond to 0.2 and 0.75 mM of Mn^{2+} per single cell, grown in TGY

264 or in manganese-supplemented medium, respectively. For cells grown for 19 h, this difference

265 does hold, the Mn^{2+} concentration being indeed equal to 0.5 and 1.45 mM for cells grown in

266 control and in manganese-supplemented medium, respectively (Supplementary Fig. S2b).

267 Accordingly, the addition of 5 µM MnCl$_2$ to TGY induces a 3-fold increase of Mn^{2+} concentration

268 *in vivo*, independently of the growth phase. This suggests that the enrichment of TGY with MnCl$_2$

269 should induce significant changes in *D. radiodurans* proteome at early stages of growth.

270 Considering the effect exerted by Mn^{2+} on cell growth, we also evaluated whether Mn^{2+} addition

271 to the medium affects the cell morphology. Among the comparisons considered, some

272 significant differences were observed (Table 1): i) at 12 h of incubation or later, the cells axes

273 of control cells were longer than those of cells grown in the presence of manganese; ii) at 20-

274 25 h of incubation, cells incubated in the presence of 250 µM manganese featured shorter axes;

275 iii) the addition of 25 or 250 µM manganese shortened the diameter of cells incubated for 12

276 or 20 h, and this effect lasted for 25 h of incubation for cells grown in the presence of 250 µM

277 manganese. The peculiar morphology of control cells does nicely correlate with the observation

278 that the growth of these cells slows down after 15 h of incubation (Fig. 1a), suggesting a

279 phenotypic link between the elongation of cells axis and the onset of stationary phase. In

280 addition, we observed a significant shortening of cells diameter in those populations featuring

281 a prolonged lag phase (Table 1, Fig. 1a). It is also important to note that no aberrant

282 morphologies were observed for any of the concentrations of Mn^{2+} tested (Fig. 3a).

283 We also determined in another experiment the cytosolic accumulation of Mn^{2+} in cells cultured

284 in the absence (control) or in the presence (5, 25 or 250 µM) of MnCl$_2$, under the same growth

285 conditions. To this aim, we used a BODIPY-based turn-on fluorescent Mn^{2+} sensor, which can

286 pass the cell membrane and bind specifically to intracellular Mn^{2+} [29]. Cells grown in the

287 absence of MnCl$_2$ show a total fluorescence equal to 45.82 ± 20.64. This signal increases 3.2

288 (146.97 ± 68.40), 3.64 (166.97 ± 85.02) and 4.91 (225.02 ± 71.69) times for the samples grown

289 in the presence of 5, 25 and 250 µM MnCl$_2$, respectively (Fig.s 3b and 3c). However, the only

290 significant difference among those detected is the divergence between the total fluorescence of

cells grown in the absence of manganese and the fluorescence levels of cells grown in manganese-enriched media (Fig. 3c). This could be due to the following reasons: i) the probe concentration is limiting; ii) most of the Mn^{2+} is bound to proteins and DNA, and therefore is not accessible to the probe. In addition, we observed that at high Mn^{2+} enrichment (250 μM) of the growth medium, the cytosolic probe bleached faster than the membrane bound.

Mn^{2+} and the proteome of Deinococcus radiodurans

Taking into account the growth-promoting effect induced in *D. radiodurans* by manganese (Fig. 1), and the concomitant accumulation *in vivo* of this divalent cation (Fig. 3), we investigated in detail the proteome of cells grown in TGY or in the same medium enriched with 5 μM Mn^{2+}. Considering the kinetics of growth in both media (Fig. 1a), we decided to harvest cells from cultures grown for 15 and 19 h. By this means, we compared the proteome of control and manganese-enriched cells when their growth phase was comparable (15 h, Fig. 1a) and when the difference in population density between the 2 cultures was well established (19 h, Fig. 1a). From each sample total proteins were extracted to perform 2D electrophoresis, and the spot patterns of the 4 gels were compared. A total of 68 spots that were absent or overexpressed (spots whose intensity was at least 2-fold higher or lower than the matched spot on the other gel) in the control or in the Mn^{2+}-treated culture were selected for MS analysis. The complete list of the proteins associated to these spots is reported in Supplementary Table ST1, where it is shown that some proteins could not be identified, and others were identified as sample contaminants (e.g. keratin in spot 19, Supplementary Table ST1). In addition, some spots were found to contain *D. radiodurans* proteins whose function is hypothetical. Excluding from further analysis the proteins not identified, and those representing contaminants or featuring hypothetical functions, a total of 52 spots was left for the comparison of the 4 proteomes considered.

14

Interestingly, among these spots we observed 5 whose electrophoretic mobility was significantly affected by the enrichment with manganese of the growth medium (Table 2, Fig.s 4 and 5). These 5 proteins isolated from manganese-enriched cultures featured higher pI values, with shifts up to 1.4 pH units (Table 2). It is important to note that the most consistent pI shift (1.4) is associated to an iron ABC transporter, the molecular mass of which was found almost invariant (Table 2). The regulation of ABC transporters by phosphorylation is well documented [34], and the importance of kinases as well as the presence of phosphorylation sites has been reported [35-37]. Accordingly, we propose that in cells grown in Mn^{2+}-enriched medium the extent of phosphorylation of the iron ABC transporter is significantly reduced when compared to that at the expense of the protein from control cells, leading to a higher pI. This would, in turn, lead to a decreased activity of the iron transporter in manganese-enriched cells. It was previously shown that the radio-resistance of *D. radiodurans* is correlated to high manganese/iron ratio, *in vivo* [17]. Accordingly, the behaviour reported here for the iron ABC transporter suggests a mechanism for the beneficial effect exerted by Mn^{2+} under physiological growth conditions. In addition, the observations listed in Table 2 suggest to attempt, with future work, the identification of post-translational modification systems affected by manganese.

When the proteomes of control and manganese-enriched cells were compared after 15 h of growth, we detected 7 and 9 proteins preferentially expressed in control (Supplementary Table ST2, Fig. 4) and in manganese-enriched (Supplementary Table ST3, Fig. 4) cells, respectively. Furthermore, by comparing the two proteomes after 19 h of growth, we identified 9 and 21 proteins selectively expressed in control (Supplementary Table ST4, Fig. 5) and in manganese-enriched (Supplementary Table ST5, Fig. 5) cells, respectively. The 46 proteins accordingly identified can be classified into 4 major groups: i) the extracellular nuclease (Gi10957459) and the ribosomal 50S L5 protein (Gi15805352) are exclusively expressed in control cells, both

after 15 and 19 h of growth (spots 1 and 11, 2 and 13, Supplementary Tables ST2 and ST4); ii)

the transcription termination/anti-termination factor NusA (Gi15806798) is selectively

expressed in manganese-enriched cells, both after 15 and 19 h of growth (spots 10 and 24,

Supplementary Tables ST3 and ST5); iii) the phage shock protein A (Gi15806486) is earlier

expressed in control cells (spots 4 and 63, Supplementary Tables ST2 and ST5); the V-type

ATPase subunit A (Gi15805727) is earlier expressed in manganese-enriched cells (spots 31 and

40, Supplementary Tables ST3 and ST4); iv) the remaining 38 proteins were peculiar of both

the medium and the growth phase (i.e. expressed in one medium only, at 15 or 19 h of growth).

Concerning the extracellular nuclease, its selective expression in control cells suggests that this

enzyme sustains the recycling of nucleotides from DNA exported into the growth medium after

oxidative damage, whose occurrence could be prevented by Mn^{2+}. This suggestion is sustained

by the observation that purine nucleoside phosphorylase, a well-known phosphate-dependent

component of the purine salvage pathway [38, 39], is also selectively expressed in control cells

(Supplementary Table ST2). To this, it could be related the concomitant selective expression in

control cells of the phosphate ABC transporter (Supplementary Table ST2). The exclusive

detection (Supplementary Tables ST2 and ST3) and the overexpression (Supplementary Tables

ST4 and ST5) of NusA in manganese-enriched cells can be related to the higher biomass yield

triggered by Mn^{2+} addition to TGY medium. Remarkably, the rate of synthesis of NusA was

quantified in *Escherichia coli* as a function of medium composition, and it was shown that the

expression of this transcriptional regulator is increased five-fold in cells grown in rich medium,

when compared to the level detected in cells grown in minimal medium [40]. The ribosomal

proteins reported in Supplementary Tables ST2-ST5 deserve a detailed comment. *D.

radiodurans* is known to contain 3 ribosomal operons [41], featuring low diversity among the

23S rRNA genes. Despite this redundancy at the genomic level, our proteomic data reported in

Supplementary Tables ST2-ST5 could erroneously suggest that control or manganese-enriched

365   *D. radiodurans* cells are devoid of a particular ribosomal protein. On the contrary, it has to be

366   noted that: i) for ribosomal protein L1 a shift in pI was detected (Table 2); ii) for the same L1

367   protein we also detected an additional spot in control cells (Supplementary Table ST2), but this

368   spot does contain a truncated form of the L1 protein (25 kDa vs. the 30 kDa of full-length

369   protein); iii) the L5 ribosomal protein is apparently expressed only by control cells

370   (Supplementary Tables ST2 and ST4); it should however be remarked that the observed pI of

371   this protein was extremely lower (4.25) than the theoretical value (9.88); therefore, it is quite

372   likely that the L5 protein associated to these spots (2 and 13) represents a post-translationally

373   modified sub-population of the total amount of this ribosomal protein; iv) a particular situation

374   was observed for the 30S ribosomal S2 protein (Supplementary Table ST5): in this case, the

375   molecular mass of the protein detected in manganese-enriched cells was determined as higher

376   (37 kDa) than the expected value (30 kDa), therefore representing a pool of S2 protein

377   exclusively modified in manganese-enriched cells.

378   It should be noted that 15 h old cells represent individuals entering the stationary phase or

379   engaged in the logarithmic phase in the absence or in the presence of additional Mn^{2+},

380   respectively (Fig. 1a). Therefore, the proteins reported in Supplementary Table ST3 should be

381   diagnostic of the competence of manganese-enriched cells to sustain additional cell cycles

382   before reaching the stationary phase. In this frame, the identification of enzymes involved in

383   peptide and amino acids metabolism (Alanine-DH, Serine-OH methyl transferase, oligo

384   endopeptidase F) seems particularly meaningful when considering that *D. radiodurans* is a

385   proteolytic bacterium [1]. Moreover, the presence in this group of the molecular chaperone

386   DnaJ, which is known to assist DnaK in the hydrolysis of ATP [42], further suggests that *D.*

387   *radiodurans* cells grown for 15 h in Mn^{2+}-enriched medium are competent in sustaining

388   additional doublings. A similar situation does likely hold for cells collected after 19 h of growth,

389   which correspond to full stationary and late-logarithmic phase for control and manganese-

390   enriched cells, respectively (Fig. 1a). Among the proteins selectively detected in manganese-

391   enriched cells, it is interesting to outline the presence of enzymes diagnostic of active

392   metabolism and growth (S-protease, protease I, translation IF-2, N-acetyl-muramoyl-L-Ala

393   amidase, Supplementary Table ST5). In addition, it should however be noted that among these

394   proteins we detected enzymes involved in stress-responses (catalase, DNA-binding stress

395   response) and in the regulation of ATP availability (adenylate kinase), diagnostic of the

396   incoming stationary phase (Fig. 1a).

CONCLUDING REMARKS

398   We have shown here that under physiological conditions the addition of Mn^{2+} to the TGY rich

399   medium stimulates the growth of *D. radiodurans*, and significantly alters the proteome of this

400   bacterium. In particular, we observed that Mn^{2+} can affect both the expression level and the

401   post-translational modification of proteins. Accordingly, future work will be devoted to identify

402   these post-translational modifications and to characterize the phenotype of *D. radiodurans*

403   strains bearing mutations at the expense of some of the proteins identified here.

404

407   **Conflicts of interest**

408   The authors declare that there are no conflicts of interest.

409

REFERENCES

1. Slade D, Radman M. Oxidative stress resistance in *Deinococcus radiodurans*. *Microbiol Mol Biol Rev* 2011;75:133-191.

2. Anderson AW, Nordan HC, Cain RF, Parrish G, Duggan D. Studies on a radio-resistant micrococcus. I. Isolation, morphology, cultural characteristics, and resistance to gamma radiation. *Food Technol* 1956;10:575-577.

3. Dean CJ, Feldschreiber P, Lett JT. Repair of X-ray damage to the deoxyribonucleic acid in *Micrococcus radiodurans*. *Nature* 1966;209:49-52.

4. Moseley BE. The isolation and some properties of radiation–sensitive mutants of *Micrococcus radiodurans*. *J Gen Microbiol* 1967;49:293-300.

5. Moseley BE. Repair of ultraviolet radiation damage in sensitive mutants of *Micrococcus radiodurans*. *J Bacteriol* 1969;97:647-652.

6. Driedger AA, James AP, Grayston MJ. Cell survival and X-ray-induced DNA degradation in *Micrococcus radiodurans*. *Radiat Res* 1970;44:835-845.

7. Burrell AD, Feldschreiber P, Dean CJ. DNA-membrane association and the repair of double breaks in X-irradiated *Micrococcus radiodurans*. *Biochim Biophys Acta* 1971;247:38-53.

8. Hariharan PV, Cerutti PA. Formation and repair of gamma-ray induced thymine damage in *Micrococcus radiodurans*. *J Mol Biol* 1972;66:65-81.

9. Bonura T, Bruce AK. The repair of single-strand breaks in a radiosensitive mutant of *Micrococcus radiodurans*. *Radiat Res* 1974;57:260-275.

10. Sweet DM, Moseley BE. The resistance of *Micrococcus radiodurans* to killing and mutation by agents which damage DNA. *Mutat Res* 1976;34:175-186.

434   11.   Hansen MT. Multiplicity of genome equivalents in the radiation-resistant bacterium

435   *Micrococcus radiodurans. J Bacteriol* 1978;134:71-75.

436   12.   Harsojo, Kitayama S, Matsuyama A. Genome multiplicity and radiation resistance in

437   *Micrococcus radiodurans. J Biochem* 1981;90:877-880.

438   13.   White O, Eisen JA, Heidelberg JF, Hickey EK, Peterson JD *et al.* Genome sequence of

439   the radioresistant bacterium *Deinococcus radiodurans* R1. *Science* 1999;286:1571-

440   1577.

441   14.   Moseley BE, Mattingly A, Shimmin M. Isolation and some properties of temperature-

442   sensitive mutants of *Micrococcus radiodurans* defective in DNA synthesis. *J Gen*

443   *Microbiol* 1972;70:399-409.

444   15.   Zharadka K, Slade D, Bailone A, Sommer S, Averbeck D *et al.* Reassembly of shattered

445   chromosomes in *Deinococcus radiodurans. Nature* 2006;443:569-573.

446   16.   Leibowitz PJ, Schwartzberg LS, Bruce AK. The in vivo association of manganese with

447   the chromosome of *Micrococcus radiodurans. Photochem Photobiol* 1976;23:45-50.

448   17.   Daly MJ, Gaidamakova EK, Matrosova VY, Vasilenko A, Zhai M *et al.* Accumulation of

449   Mn(II) in *Deinococcus radiodurans* facilitates gamma-radiation resistance. *Science*

450   2004;306:1025-1028.

451   18.   Daly MJ, Gaidamakova EK, Matrosova VY, Vasilenko A, Zhai M *et al.* Protein oxidation

452   implicated as the primary determinant of bacterial radioresistance. *PLoS Biol*

453   2007;5:e92.

454   19.   Archibald FS, Fridovich I. The scavenging of superoxide radical by manganous

455   complexes: in vitro. *Arch Biochem Biophys* 1982;214:452-463.

456   20.   Barnese K, Gralla EB, Cabelli DE, Valentine JS. Manganous phosphate acts as a

457   superoxide dismutase. *J Am Chem Soc* 2008;130:4604-4606.

458   21.   Berlett BS, Chock PB, Yim MB, Stadtman ER. Manganese(II) catalyzes the
459   bicarbonate-dependent oxidation of amino acids by hydrogen peroxide and the
460   amino acid-facilitated dismutation of hydrogen peroxide. *Proc Natl Acad Sci USA*
461   1990;87:389-393.

462   22.   He Y. High cell density production of *Deinococcus radiodurans* under optimized
463   conditions. *J Ind Microbiol Biotechnol* 2009;36:539-546.

464   23.   Zhang YM, Wong TY, Chen LY, Lin CS, Liu JK. Induction of a futile Embden-Meyerhof-
465   Parnas pathway in *Deinococcus radiodurans* by Mn: possible role of the pentose
466   phosphate pathway in cell survival. *Appl Env Microbiol* 2000;66:105-122.

467   24.   Chou FI, Tan ST. Manganese(II) induces cell division and increases in superoxide
468   dismutase and catalase activities in an aging Deinococcal culture. *J Bacteriol*
469   1990;172:2029-2035.

470   25.   Lee H, Wong T, Kuo J, Liu J. The effect of Mn(II) on the autoinducing growth inhibition
471   factor in *Deinococcus radiodurans. Prep Biochem Biotechnol* 2014;44:645-652.

472   26.   Liedert C, Peltola M, Bernhardt J, Neubauer P, Salkinoja-Salonen M. Physiology of
473   resistant *Deinococcus geothermalis* bacterium aerobically cultivated in low-
474   manganese medium. *J Bacteriol* 2012;194:1552-1562.

475   27.   Santos SP, Mitchell EP, Franquelim HG, Castanho MARB, Abreu IA *et al.* Dps from
476   *Deinococcus radiodurans*: oligomeric forms of Dps1 with distinct cellular functions
477   and Dps2 involved in metal storage. *FEBS J* 2015;282:4307-4327.

478   28.   Holland AD, Rothfuss HM, Lidstrom ME. Development of a defined medium
479   supporting rapid growth for *Deinococcus radiodurans* and analysis of metabolic
480   capacities. *Appl Microbiol Biotechnol* 2006;72:1074-1082.

481   29.   Bakthavatsalam S, Sarkar A, Rakshit A, Jain S, Kumar A *et al.* Tuning macrocycles to

482   design 'turn on' fluorescence probes for manganese(II) sensing in live cells. *Chem*

483   *Comm* 2015;51:2605-2608.

484   30.   Vischer NOE, Verheul J, Postma M, van den Berg van Saparoea B, Galli E *et al.* Cell age

485   dependent concentration of *Escherichia coli* divisome proteins analyzed with ImageJ

486   and ObjectJ. *Front Microbiol* 2015;6:586.

487   31.   Shevchenko A, Tomas H, Havliš J, Olsen JV, Mann M. In-gel digestion for mass

488   spectrometric characterization of proteins and proteomes. *Nat Protoc* 2007;1:2856-

489   2860.

490   32.   Conte E, Vincelli G, Schaaper RM, Bressanin D, Stefan A *et al.* Stabilization of the

491   *Escherichia coli* DNA polymerase III ε subunit by the θ subunit favors *in vivo* assembly

492   of the Pol III catalytic core. *Arch Biochem Biophys* 2012;523:135-143.

493   33.   Venkateswaran A, McFarlan SC, Ghosal D, Minton KW, Vasilenko A *et al.* Physiologic

494   determinants of radiation resistance in *Deinococcus radiodurans. Appl Environ*

495   *Microbiol* 2000;66:2620-2666.

496   34.   Stolarczyk EI, Reiling CJ, Paumi CM. Regulation of ABC transporter function via

497   phosphorylation by protein kinases. *Curr Pharm Biotechnol* 2011;12:621-635.

498   35.   Mayati A, Moreau A, Le Vée M, Stieger B, Denizot C *et al.* Protein kinases C-mediated

499   regulations of drug transporter activity, localization and expression. *Int J Mol Sci*

500   2017;18:764.

501   36.   Anreddy N, Gupta P, Kathawala RJ, Patel A, Wurpel JND *et al.* Tyrosine kinase

502   inhibitors as reversal agents for ABC transporter mediated drug resistance.

503   *Molecules* 2014;19:13848-13877.

504   37.   Cohen P. The role of protein phosphorylation in human health and disease. The Sir

505   Hans Krebs medal lecture. *Eur J Biochem* 2001;268:5001-5010.

506   38.   Murray AW. The biological significance of purine salvage. *Ann Rev Biochem*

507   1971;40:811-826.

508   39.   Bzowska A, Kulikowska E, Shugar D. Purine nucleoside phosphorylases: properties,

509   functions, and clinical aspects. *Pharmacol Ther* 2000;88:349-425.

510   40.   Li GW, Burkhardt D, Gross C, Weissman JS. Quantifying absolute protein synthesis

511   rates reveals principles underlying allocation of cellular resources. *Cell*

512   2014;157:624-635.

513   41.   Pei A, Nossa CW, Chokshi P, Blaser MJ, Yang L *et al.* Diversity of 23S rRNA genes

514   within individual prokaryotic genomes. *PLos ONE* 2009;4:e5437.

515   42.   Dekker SL, Kampinga HH, Bergink S. DNAJs: more than substrate delivery to HSPA.

516   *Front Mol Biosci* 2015;2:35.

517

518

FIGURE LEGENDS

520 **Figure 1**

521 Manganese and growth of *Deinococcus radiodurans*. **(a)** Growth kinetics of *D. radiodurans*

522 in TGY liquid medium (green circles) or in the same medium supplemented with 2.5, 5, 10,

523 25, or 250 μM $MnCl_2$ (blue, red, purple, dark green, and cyano circles, respectively). **(b)**

524 Population density of *D. radiodurans* cultures grown for 19 h in TGY medium (red bars) or

525 in the same medium to which 5 μM $MnCl_2$ was added (green bars), as determined

526 spectroscopically (Absorbance at 600 nm), using a Thoma chamber (Individuals/mL) or by

527 colony counting (c.f.u./mL). Diads and tetrads were considered as single individuals. The

528 error bars represent standard deviation (n = 3). The experimental mean values were

529 compared by the Student's t test (**, ***, and **** indicate P < 0.01, <0.001, <0.0001,

530 respectively).

531

532 **Figure 2**

533 Distribution of *Deinococcus radiodurans* populations among single cells, diads, and tetrads.

534 Cultures of *D. radiodurans* were grown for 19 h in TGY medium (dark green bars) or in the

535 same medium supplemented with 5 μM $MnCl_2$ (green bars), and aliquots were withdrawn

536 for direct counting with a Thoma chamber. About 300 individuals were considered for each

537 sample, and the analysis was repeated in triplicate. Error bars represent standard deviation

538 (n = 3). The experimental mean values were compared by the Student's t test (* indicates P

539 < 0.05).

540

541 **Figure 3**

542 Phenotypes of *Deinococcus radiodurans* cells grown in TGY medium supplemented or not

543 with $MnCl_2$. **(a)** Representative cells of *D. radiodurans* cells grown at 30 °C in TGY medium,

544   to which 0 (control), 5, 25 or 250 μM MnCl₂ was added; samples were harvested 0, 12, 20

545   and 25 hours after pre-cultures dilution (for a morphological analysis see Table 1). **(b)**

546   Phase contrast and fluorescence images of *D. radiodurans* cells incubated with a BODIPY-

547   based Mn^{2+} sensor. **(c)** Total Fluorescence determined in *D. radiodurans* cells as a result of

548   the accumulation of a BODIPY-based Mn^{2+} sensor that specifically binds intracellular Mn^{2+}.

549   Number of cells analyzed was 895, 1012, 622, and 235 for the control, 5, 25, and 250 μM

550   MnCl₂, respectively. Scale bar equals 2 μm. The experimental mean values were compared

551   by the Student's t test (*** indicates $P < 0.001$).

552

553   **Figure 4**

554   Manganese and the proteome of *Deinococcus radiodurans.* 2D electrophoresis of protein

555   extracts isolated from *D. radiodurans* cells grown for 15 h in TGY medium (**a**) or in the same

556   medium supplemented with 5 μM MnCl₂ (**b**). The molecular mass in kDa of the markers

557   used for the second dimension is reported on the left.

558   **Figure 5**

559   Manganese and the proteome of *Deinococcus radiodurans.* 2D electrophoresis of protein

560   extracts isolated from *D. radiodurans* cells grown for 19 h in TGY medium (**a**) or in the same

561   medium supplemented with 5 μM MnCl₂ (**b**). The molecular mass in kDa of the markers

562   used for the second dimension is reported on the left.

563   **Supplementary Figure S1**

564   Manganese and growth of *Deinococcus radiodurans*. Growth kinetics of *D. radiodurans* in

565   TGY liquid medium (green circles, squares, and triangles) or in the same medium

566   supplemented with 5 μM MnCl₂ (blue circles, squares, and triangles). The growth kinetics

567   was determined for 3 independent cultures (3 different single colonies were used) of each

568   sample (green symbols: TGY medium; blue symbols: TGY medium supplemented with 5 μM

569    $MnCl_2$). The horizontal bars represent the mean of the final Absorbance values determined

570   for the two groups of cultures (the error bars indicate standard deviation). The

571   experimental mean values were compared by the Student's t test (*** indicates $P < 0.001$).

572   **Supplementary Figure S2**

573   Manganese levels in cells of *Deinococcus radiodurans*. Cultures of *D. radiodurans* were

574   grown for 15 and 19 h (Panels a and b, respectively) in TGY medium, or in the same medium

575   supplemented with 5 μM $MnCl_2$. The content of Mn^{2+} in whole cells grown in TGY (green

576   squares) or in medium supplemented with 5 μM $MnCl_2$ (blue squares) was determined by

577   atomic absorption spectroscopy, and compared with appropriate standards (open circles).

578   The analyses were performed using 1 mL of each cell suspension (in ultrapure water). The

579   number of cells per mL was determined on sample aliquots, and the volume of a single cell

580   was assumed as equal to 8 μm^3. It should be noted that the cells volume accounted for about

581   0.1% of the sample volume. To avoid underestimation of the Mn^{2+} concentration in cells

582   grown for 19 h in manganese-enriched medium, the sample was diluted 1:2 with ultrapure
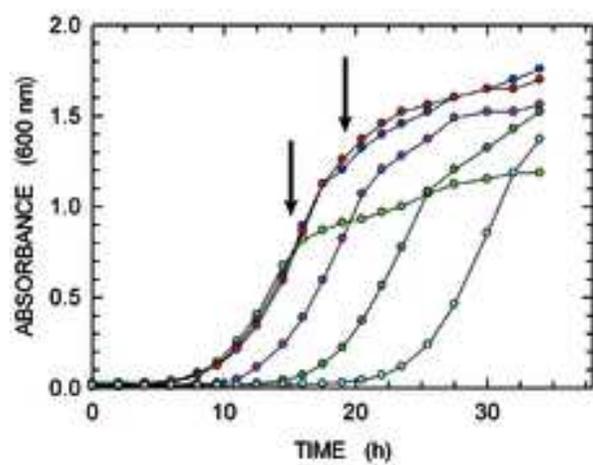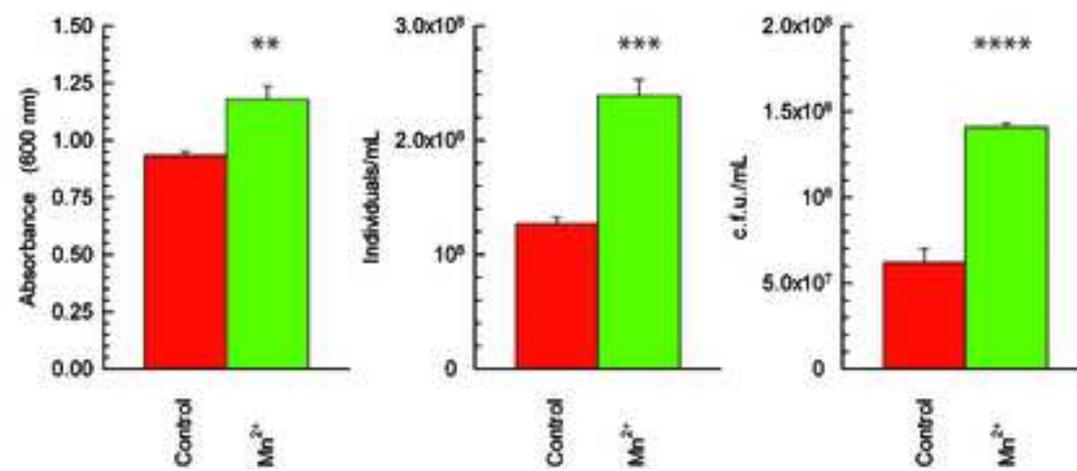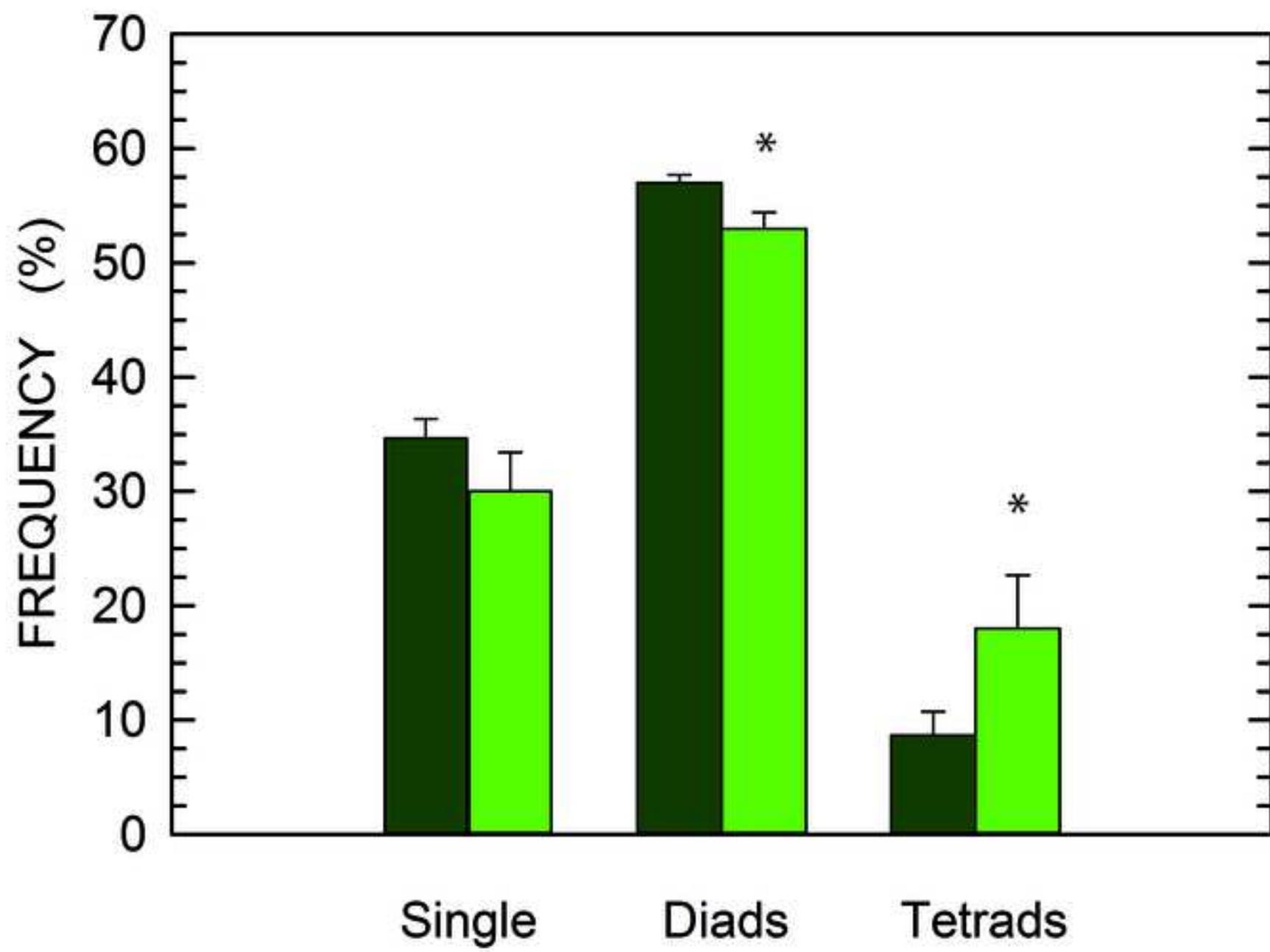
583   water.

584

585

586

Figure 1

Figure 2

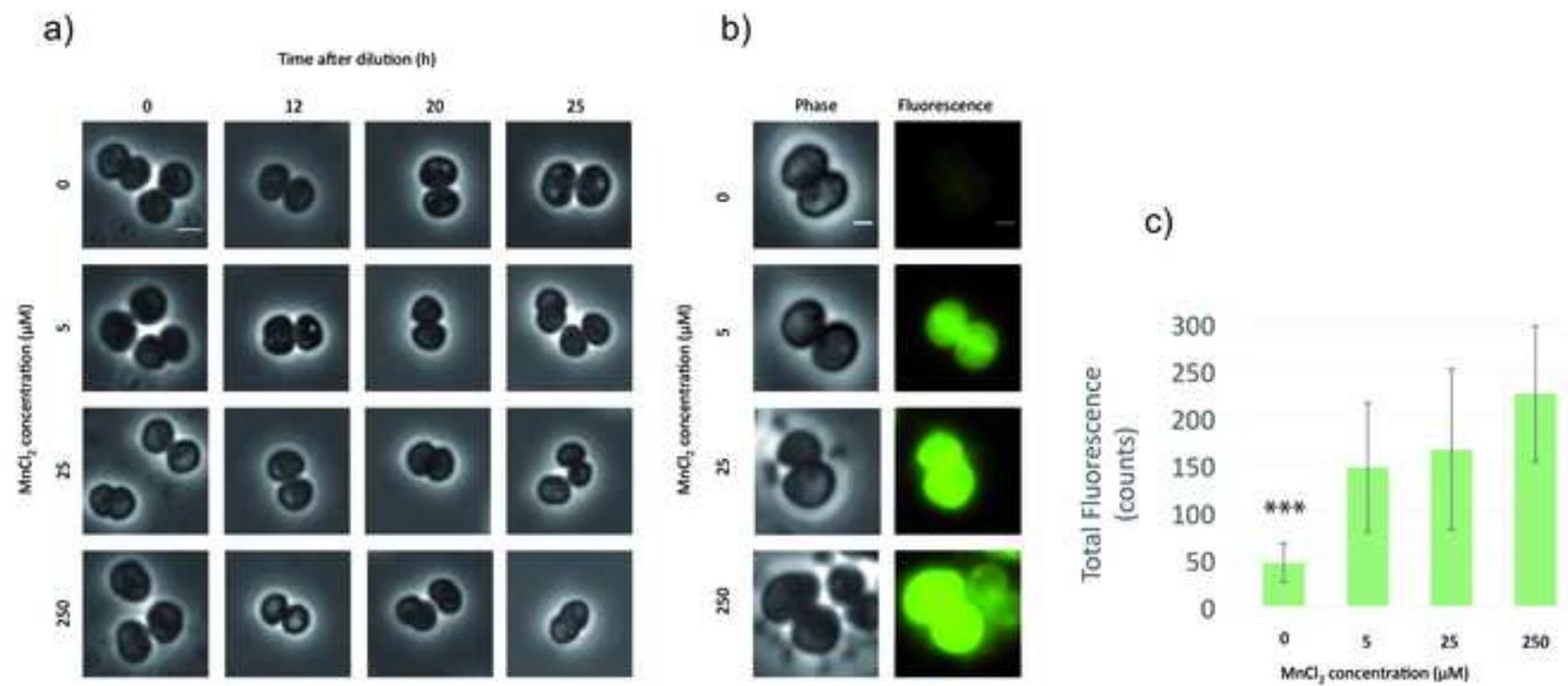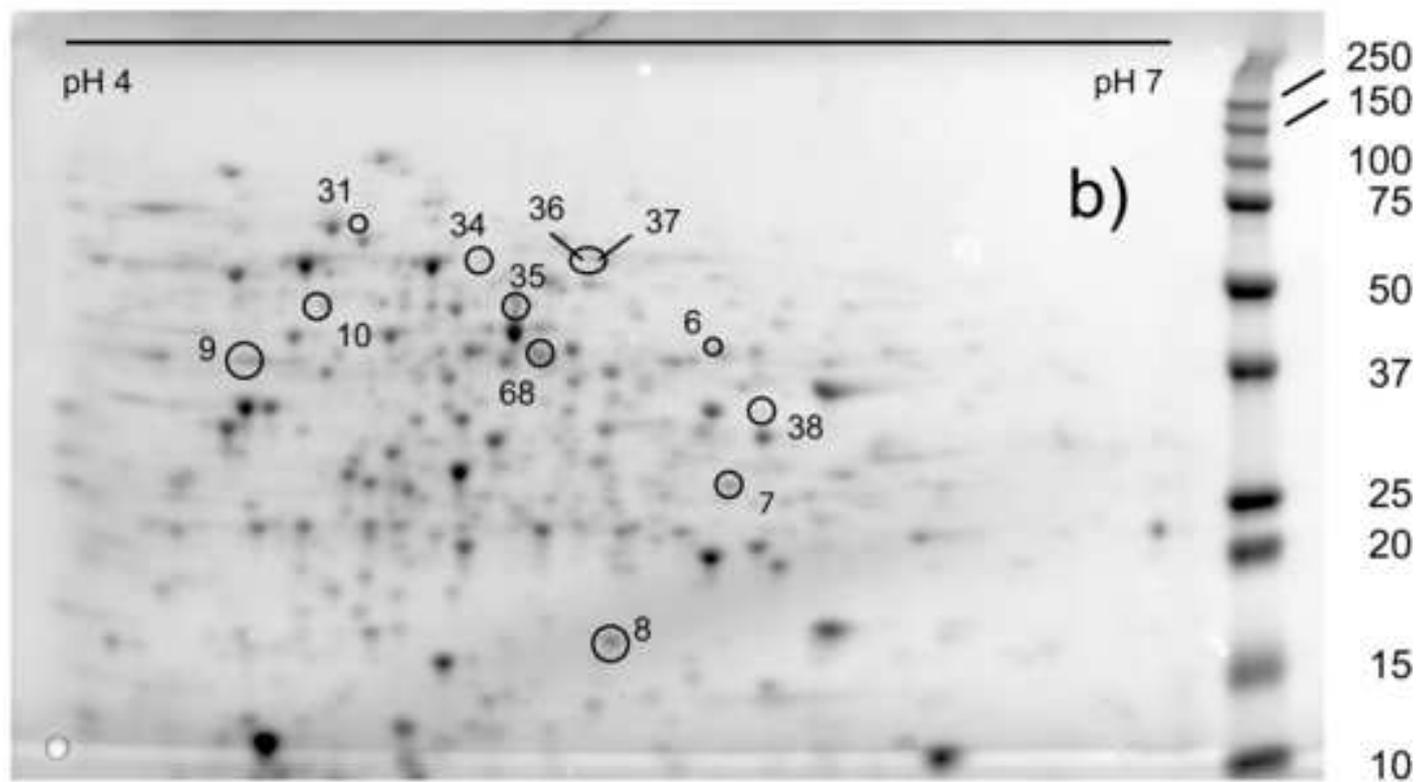Figure 3

Figure 4

Figure 5

Table 1
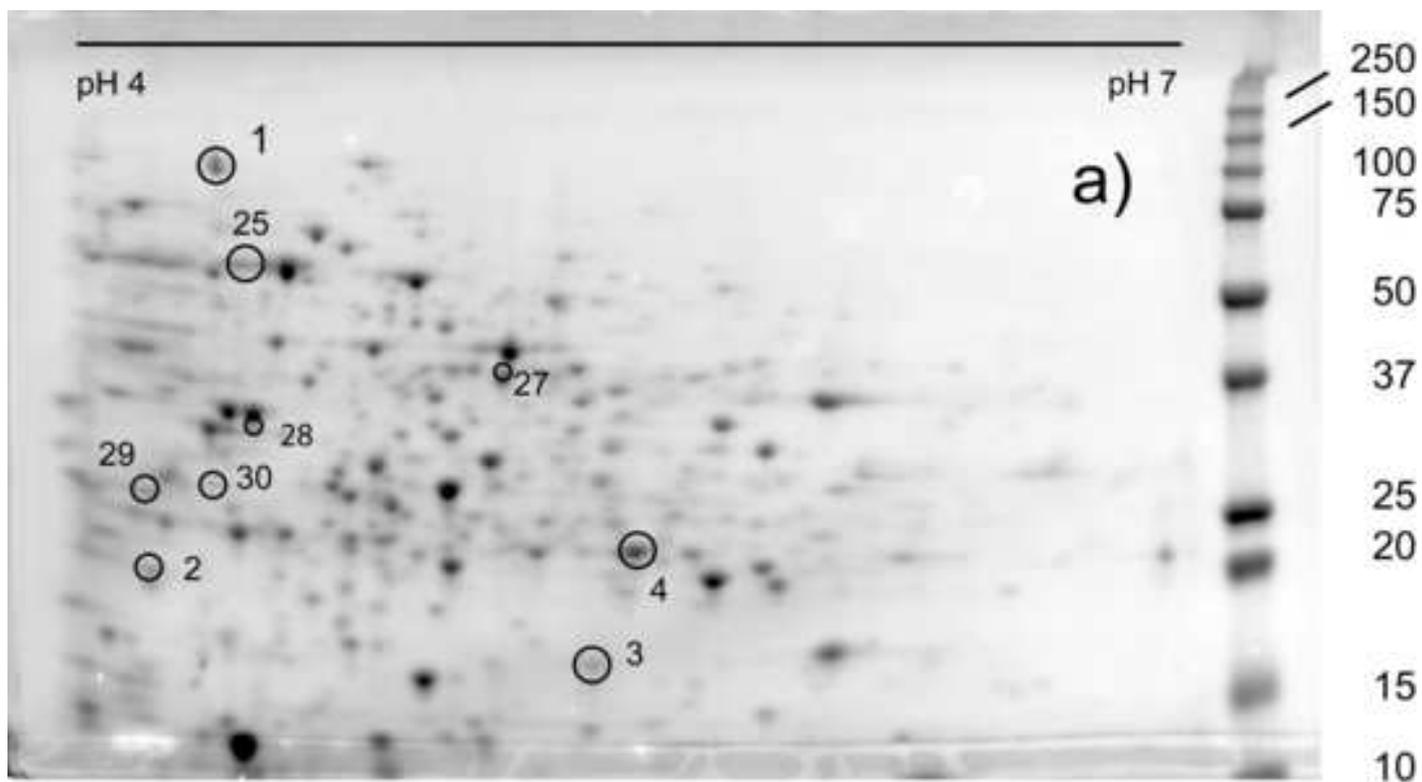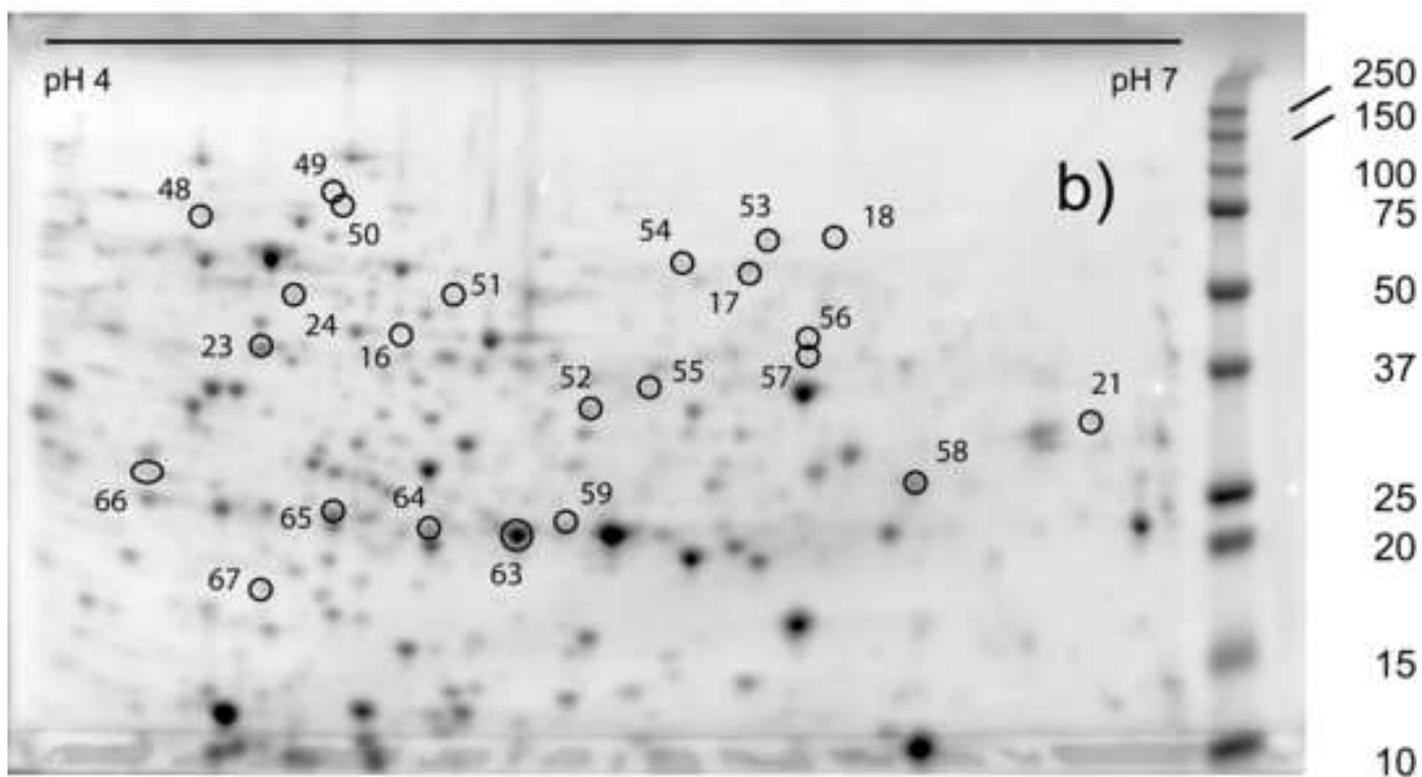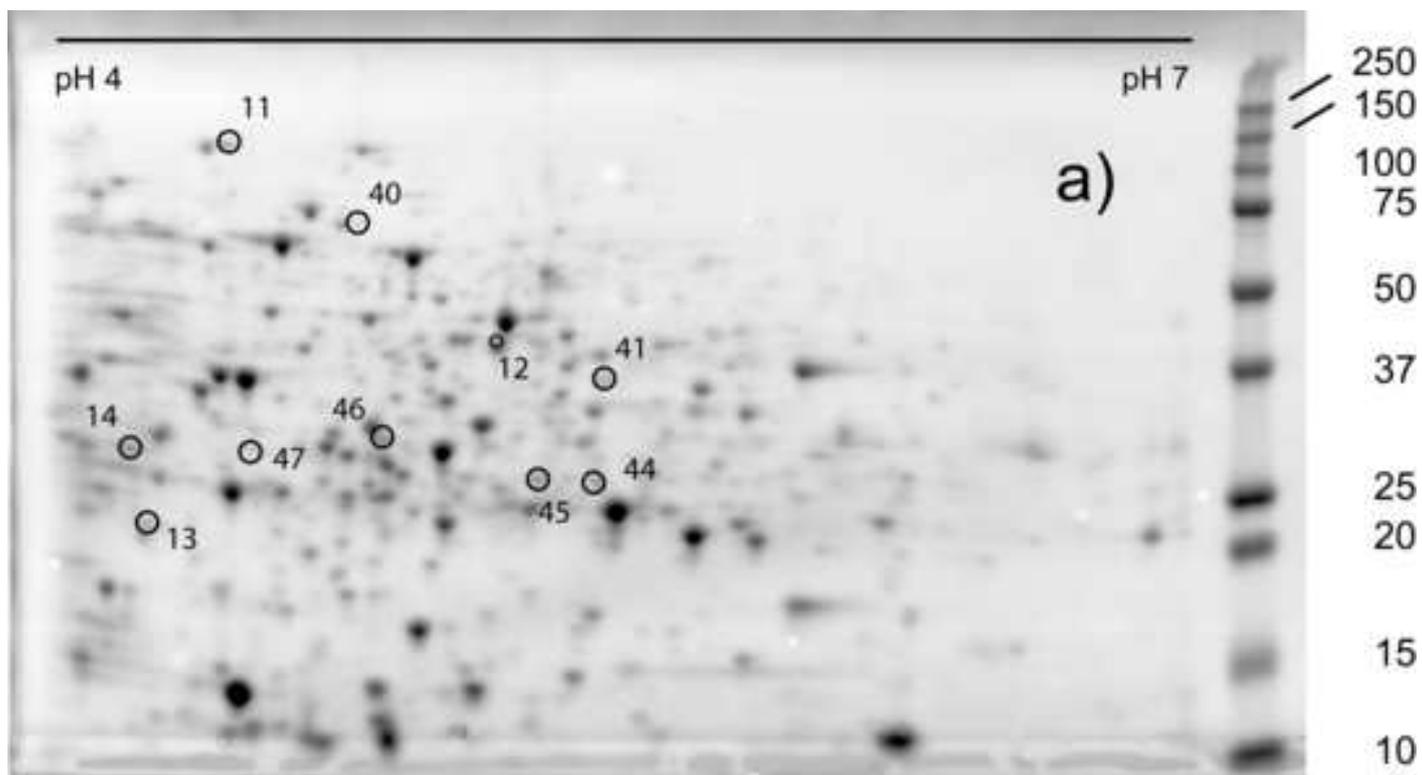
Interval	Sample	Axis	Diameter	*n*
0 h	Control	2.73 ± 0.72	2.17 ± 0.38	213
	5 μM MnCl$_2$	2.76 ± 0.33	2.17 ± 0.36	246
	25 μM MnCl$_2$	2.77 ± 0.26	2.11 ± 0.33	217
	250 μM MnCl$_2$	2.76 ± 0.33	2.22 ± 0.33	247
12 h	Control	*2.81 ± 0.37	2.23 ± 0.21	328
	5 μM MnCl$_2$	2.74 ± 0.33	2.19 ± 0.20	252
	25 μM MnCl$_2$	2.70 ± 0.34	*2.11 ± 0.16	177
	250 μM MnCl$_2$	2.66 ± 0.29	*2.08 ± 0.18	450
20 h	Control	*2.88 ± 0.37	2.20 ± 0.23	217
	5 μM MnCl$_2$	2.73 ± 0.34	2.19 ± 0.21	242
	25 μM MnCl$_2$	2.70 ± 0.29	*2.10 ± 0.24	501
	250 μM MnCl$_2$	*2.64 ± 0.27	*2.06 ± 0.33	258
25 h	Control	*2.80 ± 0.36	2.11 ± 0.29	691
	5 μM MnCl$_2$	2.69 ± 0.36	2.11 ± 0.24	600
	25 μM MnCl$_2$	2.68 ± 0.37	2.10 ± 0.28	586
	250 μM MnCl$_2$	*2.59 ± 0.32	*2.05 ± 0.23	283

Table 1

Addition of Mn^{2+} to TGY medium and morphology of *D. radiodurans* cells. Measurements of cells axis and diameter of *D. radiodurans* cells incubated in the presence of 0 (control), 5, 25 or 250 μM MnCl$_2$ for 0, 12, 20 and 25 hours after dilution in TGY medium, at 30 °C. The experimental mean values were compared by the one-way ANOVA test (* indicates P < 0.05).

Table 2

Identity	Function	Observed pI/Mr	
		-Mn	+Mn
Gi15807484 (DR_2499)	Nucleoside PPi kinase	**5.45/16** (spot 3)	**5.5/16** (spot 8)
Gi15807466 (DR_2480)	AcCoA Acetyltransferase	**5.25/40** (spot 27)	**5.36/40** (spot 68)
Gi15805338 (DR_0309)	Elongation factor Tu	**5.25/40** (spot 27)	**5.28/48** (spot 35)
Gi15807570 (DR_2588)	Iron ABC transporter	**4.38/27** (spot 30)	**5.78/26** (spot 7)
Gi15807039 (DR_2045)	50S ribosomal protein L1	**4.18/30** (spot 14)	**4.35/30** (spot 66)

Table 2

The addition of Mn^{2+} to TGY medium triggers a shift of the isoeletric points of some *D. radiodurans* proteins. Observed isoelectric points (pI) and molecular masses (Mr) of *D. radiodurans* proteins extracted from cells grown in TGY medium (-Mn) or in the same medium supplemented with 5 µM $MnCl_2$ (+Mn). The number of the spot from which proteins were extracted is indicated in brackets.